Neutrino and Dark Radiation properties in light of latest CMB observations

Maria Archidiacono,[1] Elena Giusarma,[2] Alessandro Melchiorri,[3] and Olga Mena[2]

[1]*Department of Physics and Astronomy University of Aarhus, DK-8000 Aarhus C, Denmark*
[2]*IFIC, Universidad de Valencia-CSIC, 46071, Valencia, Spain*
[3]*Physics Department and INFN, Universita' di Roma "La Sapienza", Ple. Aldo Moro 2, 00185, Rome, Italy*

Recent Cosmic Microwave Background measurements at high multipoles from the South Pole Telescope and from the Atacama Cosmology Telescope seem to disagree in their conclusions for the neutrino and dark radiation properties. In this paper we set new bounds on the dark radiation and neutrino properties in different cosmological scenarios combining the ACT and SPT data with the nineyear data release of the Wilkinson Microwave Anisotropy Probe (WMAP-9), Baryon Acoustic Oscillation data, Hubble Telescope measurements of the Hubble constant, and Supernovae Ia luminosity distance data. In the standard three massive neutrino case, the two high multipole probes give similar results if Baryon Acoustic Oscillation data are removed from the analyses and Hubble Telescope measurements are also exploited. A similar result is obtained within a standard cosmology with $N_{\rm eff}$ massless neutrinos, although in this case the agreement between these two measurements is also improved when considering simultaneously Baryon Acoustic Oscillation data and Hubble Space Telescope measurements. In the $N_{\rm eff}$ massive neutrino case the two high multipole probes give very different results regardless of the external data sets used in the combined analyses.

When considering extended cosmological scenarios with a dark energy equation of state or with a running of the scalar spectral index, the evidence for neutrino masses found for the South Pole Telescope in the three neutrino scenario disappears for all the data combinations explored here. Again, adding Hubble Telescope data seems to improve the agreement between the two high multipole CMB measurements considered here. In the case in which a dark radiation background with unknown clustering properties is also considered, SPT data seem to exclude the standard value for the dark radiation viscosity $c^2_{\rm vis} = 1/3$ at the 2σ CL, finding evidence for massive neutrinos only when combining SPT data with BAO measurements.

PACS numbers: 98.80.-k 95.85.Sz, 98.70.Vc, 98.80.Cq

I. INTRODUCTION

Solar, atmospheric, reactor, and accelerator neutrinos have provided compelling evidence for the existence of neutrino oscillations. Barring exotic explanations, oscillation data imply non-zero neutrino masses. However, oscillation experiments only provide bounds on the neutrino mass squared differences, and therefore the measurement of the absolute scale of the neutrino mass must come from different observations. In the Standard Model of elementary particles, there are three active neutrinos. However, additional sterile neutrino species, or extra relativistic degrees of freedom could also arise in a number of extensions to the standard model of particle physics, as for instance, in axion models [1], in decaying of non-relativistic matter models [2], in scenarios with gravity waves [3], extra dimensions [4], early dark energy [5] or in asymmetric dark matter models [6]. Cosmological data provide a tool to test the neutrino properties, since the neutrino masses and abundances affect both the Cosmic Microwave Background (CMB) physics as well as the galaxy clustering properties, see Refs [7–24] for constraints on the neutrino masses and/or abundances with a variety of cosmological data sets and different assumptions regarding the fiducial cosmology.

On the other hand, cosmological measurements also allow to test the clustering properties of the extra relativistic degrees of freedom, parameterized via $N_{\rm eff}$, being $N_{\rm eff} = 3.04$ in the standard model scenario. The clustering pattern of the dark radiation component is represented by its rest frame speed of sound $c^2_{\rm eff}$ and its viscosity parameter $c^2_{\rm vis}$. The former parameter controls the relationship between velocity and anisotropic stress, being these parameters $c^2_{\rm eff} = c^2_{\rm vis} = 1/3$ if the dark radiation background is composed by neutrinos. Several analyses have set bounds on these parameters [25–27] under different assumptions regarding the underlying cosmological model.

Recently new CMB data have become available. The Wilkinson Microwave Anisotropy Probe (WMAP) collaboration has presented the cosmological implications of their final nine–year data release [28], finding $\sum m_\nu < 0.44$ eV at the 95% CL and $N_{\rm eff} = 3.84 \pm 0.40$ (being $N_{\rm eff}$ the number of thermalised massless neutrino species) when they combine their data with CMB small scale measurements (as those from previous data releases from both the Atacama Cosmology Telescope ACT [29] and the South Pole Telescope SPT [30]), Baryon Acoustic Oscillations (BAO) and Hubble Space Telescope (HST) measurements.

The SPT collaboration has also recently presented their observations of 2540 deg^2 of sky, providing the CMB temperature anisotropy power over the multipole range $650 < \ell < 3000$ [31, 32], corresponding to the region from the third to the ninth acoustic peak. The SPT measurements have found evidence for a decreasing power at high multipoles relative to the predictions within a ΛCDM scenario, which suggest, potentially, that exten-

sions to the minimal ΛCDM scenario might be needed. In the case in which massive neutrinos are added in the cosmological data analyses, the SPT collaboration finds that the combination of SPT data with WMAP (7 year data), together with Baryon Acoustic Oscillation (BAO) and Hubble Space Telescope (HST) measurements shows a 2σ preference for these models (when compared to the ΛCDM scenario). In the case of three active massive neutrinos, they find $\sum m_\nu = 0.32 \pm 0.11$ after considering CMB, BAO, HST and SPT cluster measurements. However, if the BAO measurements are removed and only CMB and HST data are considered, the evidence for neutrino masses disappears at the 95% CL. The authors of Ref. [31] also find that when a curvature component or a running in the spectral index of the primordial perturbation spectrum are added as free parameters together with $\sum m_\nu$, the preference for nonzero neutrino masses is significantly reduced. When $N_{\rm eff}$ massless neutrinos are considered, the bounds are $N_{\rm eff} = 3.71 \pm 0.35$ for the combination of CMB, BAO and HST data sets. Finally, when allowing for $N_{\rm eff}$ massive neutrino species the bounds are $\sum m_\nu = 0.51 \pm 0.15$ eV and $N_{\rm eff} = 3.86 \pm 0.37$, implying a $\sim 3\sigma$ preference for $\sum m_\nu > 0$ and a 2.2σ preference for $N_{\rm eff} > 3.046$.

These findings, if confirmed by future CMB observations, as those by the ongoing Planck mission [33], have an enormous impact for Majorana neutrino searches. The mean value for $\sum m_\nu$ found by the SPT collaboration implies a quasi-degenerate neutrino spectrum and therefore the discovery of the neutrino character becomes at reach at near future neutrinoless double beta decay experiments [34].

However, and also recently, the ACT collaboration has released new measurements of the CMB damping tail [35], finding a much lower value for $N_{\rm eff} = 2.79 \pm 0.56$ when combining with WMAP 7 year data. When considering also BAO and HST measurements, the value is higher, $N_{\rm eff} = 3.50 \pm 0.42$.

The two data sets, SPT and ACT, seem also to disagree in the value of the lensing amplitude parameter A_L at more than 95% CL [36]. On the other hand, ACT data do not seem to see evidence for neutrino masses, placing un upper limit of $\sum m_\nu < 0.39$ eV at 95% CL when ACT data are combined with WMAP 7 year data together with BAO and HST measurements.

We explore here the cosmological constraints in several neutrino and dark radiation scenarios including the new WMAP 9 year data as well as the new SPT and ACT measurements at high multipoles ℓ. We also consider the impact of other cosmological data sets, as BAO, HST and Supernova Ia luminosity distance measurements. We start with the massive neutrino case within a ΛCDM scenario, setting bounds first on $\sum m_\nu$ assuming three massive neutrinos and then moving to the case in which there are $N_{\rm eff}$ massive species with a total mass given by $\sum m_\nu$. We then enlarge the minimal ΛCDM scenario allowing for more general models with a constant dark energy equation of state or with a running of the scalar spectral index. We continue by studying the dark radiation properties, focusing first on the thermal abundances $N_{\rm eff}$ and adding after the dark radiation clustering properties $c^2_{\rm vis}$ and $c^2_{\rm eff}$ as free parameters in the analysis.

The structure of the paper is as follows. In Sec. II we describe the data sets used in the numerical analyses as well as the cosmological parameters used in each of the neutrino and dark radiation models examined in Sec. III. We draw our conclusions in Sec. IV.

II. DATA AND COSMOLOGICAL PARAMETERS

The standard, three massive neutrino scenario we explore here is described by the following set of parameters:

$$\{\omega_b, \omega_c, \Theta_s, \tau, n_s, \log[10^{10} A_s], \sum m_\nu\} \ , \qquad (1)$$

being $\omega_b \equiv \Omega_b h^2$ and $\omega_c \equiv \Omega_c h^2$ the physical baryon and cold dark matter energy densities, Θ_s the ratio between the sound horizon and the angular diameter distance at decoupling, τ is the reionization optical depth, n_s the scalar spectral index, A_s the amplitude of the primordial spectrum and $\sum m_\nu$ the sum of the masses of the three active neutrinos in eV. We assume a degenerate neutrino mass spectrum in the following. The former scenario is enlarged with $N_{\rm eff}$ massive neutrinos in the case of extended models

$$\{\omega_b, \omega_c, \Theta_s, \tau, n_s, \log[10^{10} A_s], N_{\rm eff}, \sum m_\nu\} \ , \qquad (2)$$

or with a constant dark energy equation of state w (or with a running of the scalar spectral index $n_{\rm run}$) when considering more general cosmological models:

$$\{\omega_b, \omega_c, \Theta_s, \tau, n_s, \log[10^{10} A_s], w(n_{\rm run}), \sum m_\nu\} \ . \qquad (3)$$

We also study dark radiation models, described by $\Delta N_{\rm eff}$ relativistic (i.e..massless) degrees of freedom together with three massive neutrinos with $\sum m_\nu = 0.3$ eV. This first dark radiation scheme is described by

$$\{\omega_b, \omega_c, \Theta_s, \tau, n_s, \log[10^{10} A_s], \Delta N_{\rm eff}\} \ . \qquad (4)$$

Then we also consider extended parameter scenarios, with $c^2_{\rm eff}$ and $c^2_{\rm vis}$ also as free parameters:

$$\{\omega_b, \omega_c, \Theta_s, \tau, n_s, \log[10^{10} A_s], \Delta N_{\rm eff}, c^2_{\rm vis}, c^2_{\rm eff}\} \ , \qquad (5)$$

as well as the more general case in which the sum of the three neutrino masses is also fitted to the data:

$$\{\omega_b, \omega_c, \Theta_s, \tau, n_s, \log[10^{10} A_s], \Delta N_{\rm eff}, c^2_{\rm vis}, c^2_{\rm eff}, \sum m_\nu\} \ , \qquad (6)$$

For our numerical analyses, we have used the Boltzmann CAMB code [37] and extracted cosmological parameters from current data using a Monte Carlo Markov Chain (MCMC) analysis based on the publicly available MCMC

package `cosmomc` [38]. Table I specifies the priors considered on the different cosmological parameters. Our neutrino mass prior is cast in the form of a (uniform) prior on the neutrino density fraction $f_\nu = \Omega_\nu/\Omega_{\rm DM}$, where Ω_ν is the ratio of the neutrino energy density over the critical density at redshift zero, and $\Omega_{\rm DM}$ is the same ratio, but for the total dark matter density, which includes cold dark matter and neutrinos.

Parameter	Prior
$\Omega_b h^2$	$0.005 \to 0.1$
$\Omega_c h^2$	$0.01 \to 0.99$
Θ_s	$0.5 \to 10$
τ	$0.01 \to 0.8$
n_s	$0.5 \to 1.5$
$\ln(10^{10} A_s)$	$2.7 \to 4$
f_ν	$0 \to 0.2$
$N_{\rm eff}$	$1.047 \to 10$
	$(0 \to 10)$
w	$-2 \to 0$
$n_{\rm run}$	$-0.07 \to 0.02$

TABLE I: Uniform priors for the cosmological parameters considered here.

Our baseline data set is the nine–year WMAP data [28] (temperature and polarization) with the routine for computing the likelihood supplied by the WMAP team. We then also add CMB data from the SPT experiment [31, 32]. In order to address for foreground contributions, the SZ amplitude A_{SZ}, the amplitude of the clustered point source contribution, A_C, and the amplitude of the Poisson distributed point source contribution, A_P, are added as nuisance parameters in the CMB data analyses. Separately, we also consider data from the ACT CMB experiment [35], in order to check the constraints on neutrino and dark radiation properties with the combination of both WMAP plus SPT data sets and WMAP plus ACT data sets. To the CMB basic data sets we add the latest constraint on the Hubble constant H_0 from the Hubble Space Telescope (HST) [39], or supernova data from the 3 year Supernova Legacy Survey (SNLS3), see Ref. [40]. We do not consider the combination of HST and SNLS3 measurements because these two data sets are not totally independent. In the case of SNLS3 data, we add in the MCMC analysis two extra nuisance parameters related to the light curve fitting procedure used to analyse the supernova (SN) data. These parameters characterise the dependence of the intrinsic supernova magnitude on stretch (which measures the shape of the SN light curve) and color [40]. Galaxy clustering measurements are considered in our analyses via BAO signals. We use here the BAO signal from DR9 [41] of the Baryon Acoustic Spectroscopic Survey (BOSS) [42, 43], with a median redshift of $z = 0.57$. Together with the CMASS DR9 data, we also include the recent measurement of the BAO scale based on a re-analysis (using reconstruction [44]) of the LRG sample from Data Release 7 with a median redshift of $z = 0.35$ [45], the measurement of the BAO signal at a lower redshift $z = 0.106$ from the 6dF Galaxy Survey 6dFGS [46] and the BAO measurements from the WiggleZ Survey at $z = 0.44$, $z = 0.6$ and $z = 0.73$ [47]. The data combinations for which we will show results in the next section are the following: WMAP and SPT/ACT; WMAP, SPT/ACT and HST; WMAP, SPT/ACT and SNLS3; WMAP, SPT/ACT and BAO; WMAP, SPT/ACT, HST and BAO; and finally WMAP, SPT/ACT, SNLS3 and BAO.

III. RESULTS

Here we present the constraints from current cosmological data sets on the neutrino thermal abundance $N_{\rm eff}$ and on the sum of their masses $\sum m_\nu$ in different scenarios, considering separately SPT and ACT CMB data sets.

A. Standard Cosmology plus massive neutrinos

Through this section we shall assume a ΛCDM cosmology with either three or $N_{\rm eff}$ light massive neutrinos. The left panels of Figs. 1 and 2, depict our results for the three and $N_{\rm eff}$ massive neutrino assumptions, respectively, in the case of considering SPT CMB data, combined with the other data sets exploited here. Tables II and III present the mean values and errors (or 95% CL bounds) in the three and $N_{\rm eff}$ massive neutrino scenarios in the case of considering SPT for the different data combinations detailed in the previous section. Our results agree with those presented in Ref. [31] by the SPT collaboration. Notice that BAO data are crucial for the preference for massive neutrinos in the three massive neutrino case, in which $\sum m_\nu = 0.33 \pm 0.17$ ($\sum m_\nu = 0.40 \pm 0.18$ eV) for CMB plus BAO plus HST (SNLS3) data. In the $N_{\rm eff}$ massive neutrino scenario, the bounds are $\sum m_\nu = 0.56 \pm 0.23$ eV and $N_{\rm eff} = 4.21 \pm 0.46$ ($\sum m_\nu = 0.50 \pm 0.21$ eV and $N_{\rm eff} = 3.87 \pm 0.68$) for CMB plus BAO plus HST (SNLS3) data.

If BAO data are removed, the preference for massive neutrinos disappears in the three massive neutrino case, with a 95% CL upper limit on the sum of the three active neutrinos of $\sum m_\nu < 0.50$ eV in the case of considering WMAP, SPT and HST measurements. For the same combination of data sets, in the $N_{\rm eff}$ massive neutrino case explored here, $\sum m_\nu = 0.48 \pm 0.33$ eV and $N_{\rm eff} = 4.08 \pm 0.54$.

We then consider separately new ACT data and perform identical analyses to the ones done with SPT data, see Tabs. IV, V. Figures 1 and 2 (right panels) depict our results for the three and $N_{\rm eff}$ massive neutrino assumptions, respectively, in the case of considering ACT CMB data combined with the other data sets described in the previous section. Notice that there is no evidence for neutrino masses in any of the data combinations ex-

plored here. A 95% CL upper limit on the sum of the neutrino masses of $\sum m_\nu < 0.44$ eV (< 0.54 eV) is found when considering CMB, BAO and HST (SNLS3) data, which agrees with the results presented in Ref. [35]. In the $N_{\rm eff}$ massive neutrino case, we find $\sum m_\nu < 0.50$ eV ($\sum m_\nu < 0.53$ eV) at 95% CL and $N_{\rm eff} = 3.44 \pm 0.37$ ($N_{\rm eff} = 2.77 \pm 0.46$) when considering CMB, BAO and HST (SNLS3) data. Only when adding HST measurements the allowed values of $N_{\rm eff}$ are larger than 3, see Tab. V, bringing the mean value of $N_{\rm eff}$ closer to the one found in the SPT data analyses. When removing BAO data, we get $\sum m_\nu < 0.34$ eV (95% CL) for the combination of CMB and HST measurements in the three massive neutrino case and $\sum m_\nu < 0.39$ eV (95% CL), $N_{\rm eff} < 3.20 \pm 0.38$ in the $N_{\rm eff}$ massive neutrino case.

Therefore, we conclude that, within a standard cosmology with three massive neutrinos, ACT and SPT CMB measurements are compatible if BAO data are not considered in the analyses and if a prior on H_0 from the HST experiment is also considered. However, the predictions in the $N_{\rm eff}$ massive neutrino case arising from ACT and SPT data are not consistent even if BAO data are removed and a prior on H_0 from the HST experiment is also added.

B. Massive neutrinos and extended cosmologies

In this section we compute the bounds on the sum of the three active neutrino masses considering extended cosmologies with a dark energy equation of state or with a running of the scalar spectral index.

Concerning the dark energy equation of state w, there is a strong and very well known degeneracy among the sum of neutrino masses and the dark energy equation of state w, see Ref. [48]. The bounds from cosmology on the sum of the neutrino masses will be much weaker if the dark energy fluid is not interpreted as a cosmological contant, in which case, the dark energy equation of state will be an extra free parameter. If w is allowed to vary, $\Omega_{\rm dm}$ can be much higher and consequently the neutrino mass also increases to leave unchanged the matter power spectrum and the growth of matter perturbations. The SPT collaboration [31] has also considered the impact of a constant dark energy equation of state w, and they find $\sum m_\nu = 0.27 \pm 0.11$ eV for the combination of their CMB and clusters data with WMAP 7 year, HST and BAO data sets. Figure 3, left panel, shows our results for SPT data within the different combinations of data sets addressed here. Notice that, in general, the evidence for neutrino masses in much milder than in the cosmological constant case, and the bounds on $\sum m_\nu$ are much larger than those shown in Tab. II due to the degeneracy between $\sum m_\nu$ and w. Supernovae measurements are, for this particular case, more useful than the H_0 prior from the HST experiment. Figure 3, right panel, shows the constraints in the ($\sum m_\nu$ (eV), w) plane in the case of considering ACT data. Notice that the bounds on $\sum m_\nu$ are tighter than those found for the case of analysing SPT data. Indeed, the bounds on the sum of the three massive neutrino masses computed for the case of a dark energy equation of state $w \neq -1$ are not very different from those obtained for a ΛCDM universe, see Tab. IV. SNLS3 measurements have a much larger constraining power than the HST prior also in the ACT data analyses performed in this section, especially for measuring the dark energy equation of state w.

We also explore the case in which a running in the spectral index of primordial perturbations is added to the minimal ΛCDM cosmology. In general, the spectrum of the scalar perturbations is not exactly a power law but it varies with scale. Therefore one must consider the scale dependent running of the spectral index $n_{\rm run} = dn_s/d\ln k$. Following [49], the power spectrum for the scalar perturbations reads

$$P(k) \equiv A_s k^{n(k)} \propto \left(\frac{k}{k_0}\right)^{n_s + \ln(k/k_0)(dn/d\ln k) + \cdots} ,$$

being $k_0 = 0.002$ Mpc^{-1} the pivot scale. Figure 4, left panel, shows our results for SPT data within the different combinations of data sets addressed here. The evidence for neutrino masses found for the SPT data in the cosmological constant case disappears in all the data combinations explored here. We find, for the case of the SPT data analyses, a 2σ preference for a negative running, in agreement with the results presented in Ref. [31].

Figure 4, right panel, shows our results for ACT data in the case of considering a running in the scalar spectral index. The bounds on the sum of the three massive neutrinos are now very similar to those found for the SPT experiment and also very similar to those found for ACT in the case of the minimal ΛCDM scenario. However, the preferred region for $n_{\rm run}$ is perfectly consistent with no running of the scalar spectral index, in agreement with the results presented by the ACT team [35].

C. Standard cosmology plus dark radiation

In this section we explore the bounds on the $N_{\rm eff}$ parameter, neglecting light neutrino masses and therefore assuming that there exist in nature $N_{\rm eff}$ massless neutrino species. The left (right) panel of Fig. 5 shows the constraints in the ($\Omega_{\rm dm}h^2$, $N_{\rm eff}$) plane arising from the combination of WMAP plus SPT (ACT) as well as the other data combinations shown in the previous sections. Notice that the mean value of $N_{\rm eff}$ is, in general, much higher in the case of the SPT data analyses. When considering CMB data only, $N_{\rm eff} = 3.93 \pm 0.68$ for the case of WMAP plus SPT data, while $N_{\rm eff} = 2.74 \pm 0.47$ if analysing WMAP and ACT data. The tension among these two $N_{\rm eff}$ mean values gets diluted if BAO data and a prior on H_0 from the HST experiment are added in the analyses. In that case, $N_{\rm eff} = 3.83 \pm 0.41$ ($N_{\rm eff} = 3.43 \pm 0.36$) for WMAP plus SPT (ACT), being these two measurements

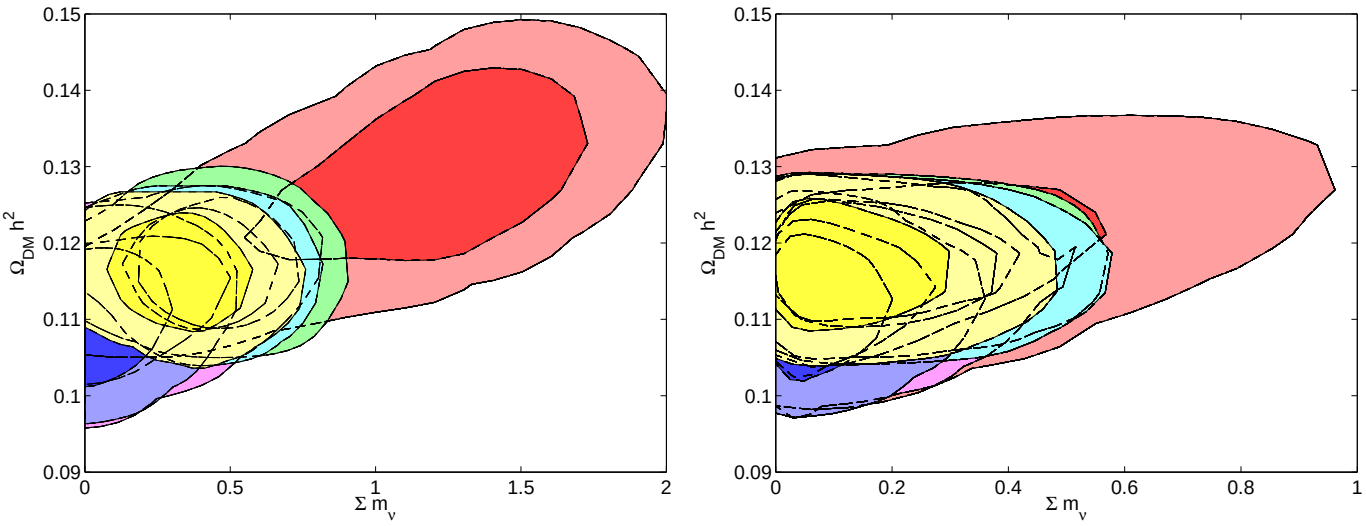

FIG. 1: Left panel (Three massive neutrino case): the red contours show the 68% and 95% CL allowed regions from the combination of WMAP and SPT measurements in the ($\sum m_\nu$ (eV), $\Omega_{\rm dm} h^2$) plane, while the magenta (blue) ones show the impact of the addition of SNLS3 (HST) data sets. The green contours depict the results from the combination of CMB and BAO data, while the cyan and yellow ones show the impact of the SNLS3 (HST) data combined with CMB and BAO measurements. Right panel: as in the left panel but considering ACT data instead of SPT.

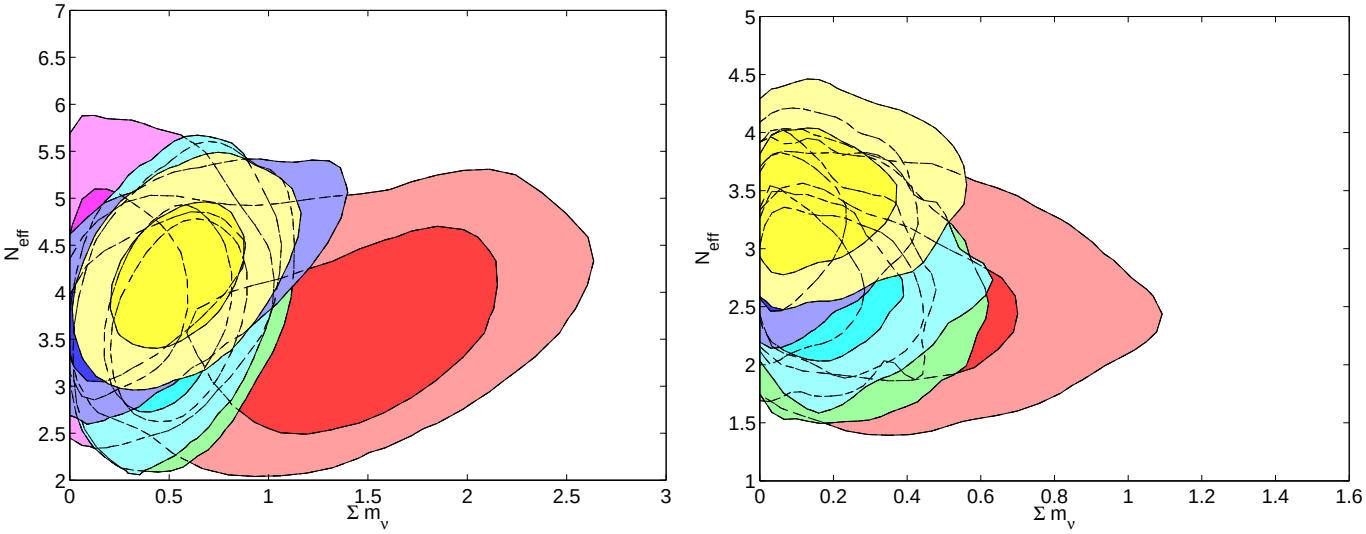

FIG. 2: Left panel ($N_{\rm eff}$ massive neutrino case): the red contours show the 68% and 95% CL allowed regions from the combination of WMAP and ACT measurements in the ($\sum m_\nu$ (eV), $N_{\rm eff}$) plane, while the magenta (blue) ones show the impact of the addition of SNLS3 (HST) data sets. The green contours depict the results from the combination of CMB and BAO data, while the cyan and yellow ones show the impact of the SNLS3 (HST) data combined with CMB and BAO measurements. Right panel: as in the left panel but considering ACT data instead of SPT.

	W9+SPT	W9+SPT + HST	W9+SPT +BAO	W9+SPT +SNLS3	W9+SPT +BAO+HST	W9+SPT +BAO+SNLS3
$\sum m_\nu$ (eV)	1.14 ± 0.41	< 0.50	0.46 ± 0.18	< 0.80	0.33 ± 0.17	0.40 ± 0.18

TABLE II: Mean values and errors (or 95% CL upper bounds) on $\sum m_\nu$ (in eV) in a standard cosmology with three massive neutrinos for the different combinations of data sets in the case of considering SPT high multipole data.

	W9+SPT	W9+SPT + HST	W9+SPT +BAO	W9+SPT +SNLS3	W9+SPT +BAO+HST	W9+SPT +BAO+SNLS3
$N_{\rm eff}$	3.66 ± 0.61	4.08 ± 0.54	3.76 ± 0.67	4.04 ± 0.68	4.21 ± 0.46	3.87 ± 0.68
$\sum m_\nu$ (eV)	1.35 ± 0.55	0.48 ± 0.33	0.56 ± 0.22	< 0.91	0.56 ± 0.23	0.50 ± 0.21

TABLE III: Mean values and errors(or 95% CL bounds) on $N_{\rm eff}$ and $\sum m_\nu$ (in eV) in a standard cosmology with $N_{\rm eff}$ massive neutrinos for the different combinations of data sets in the case of considering SPT high multipole data.

	W9+ACT	W9+ACT + HST	W9+ACT +BAO	W9+ACT +SNLS3	W9+ACT +BAO+HST	W9+ACT +BAO+SNLS3
$\sum m_\nu$ (eV)	< 0.89	< 0.34	< 0.53	< 0.49	< 0.44	< 0.54

TABLE IV: 95% CL upper bounds on $\sum m_\nu$ (in eV) in a standard cosmology with three massive neutrinos for the different combinations of data sets in the case of considering ACT high multipole data.

	W9+ACT	W9+ACT + HST	W9+ACT +BAO	W9+ACT +SNLS3	W9+ACT +BAO+HST	W9+ACT +BAO+SNLS3
$N_{\rm eff}$	2.64 ± 0.51	3.20 ± 0.38	2.63 ± 0.48	2.75 ± 0.44	3.44 ± 037	2.78 ± 0.46
$\sum m_\nu$ (eV)	< 0.95	< 0.39	< 0.55	< 0.44	< 0.50	< 0.53

TABLE V: Mean values and errors on $N_{\rm eff}$ and 95% CL upper bounds on $\sum m_\nu$ (in eV) in a standard cosmology with $N_{\rm eff}$ massive neutrinos for the different combinations of data sets in the case of considering ACT high multipole data.

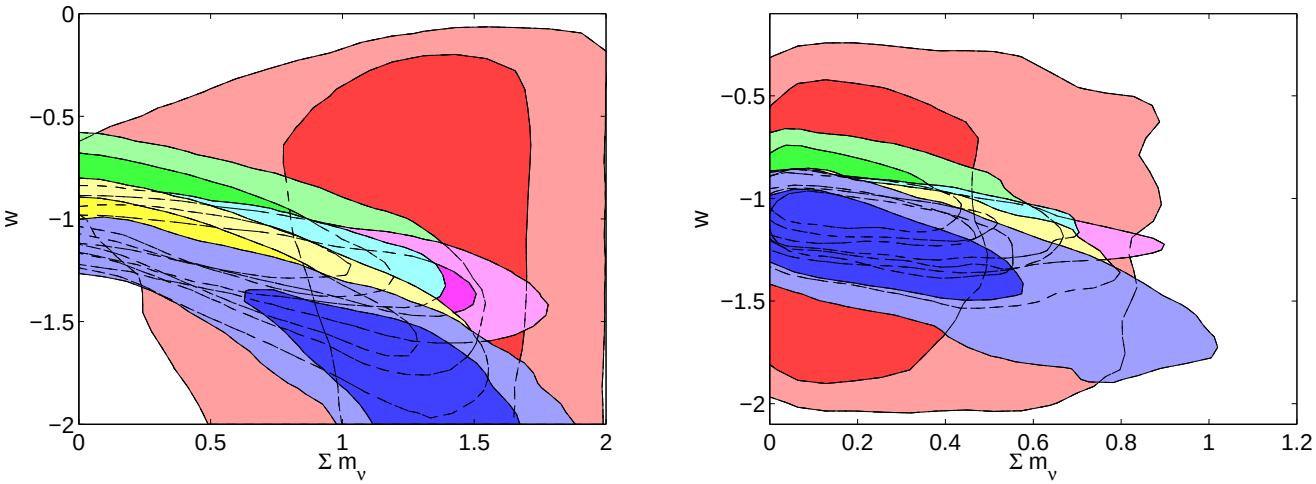

FIG. 3: Left panel (Three massive neutrino case plus dark energy): the red contours show the 68% and 95% CL allowed regions from the combination of WMAP and SPT measurements in the ($\sum m_\nu$ (eV), w) plane, while the magenta (blue) ones show the impact of the addition of SNLS3 (HST) data sets. The green contours depict the results from the combination of CMB and BAO data, while the cyan and yellow ones show the impact of the SNLS3 (HST) data combined with CMB and BAO measurements. Right panel: as in the left panel but for the case of ACT data.

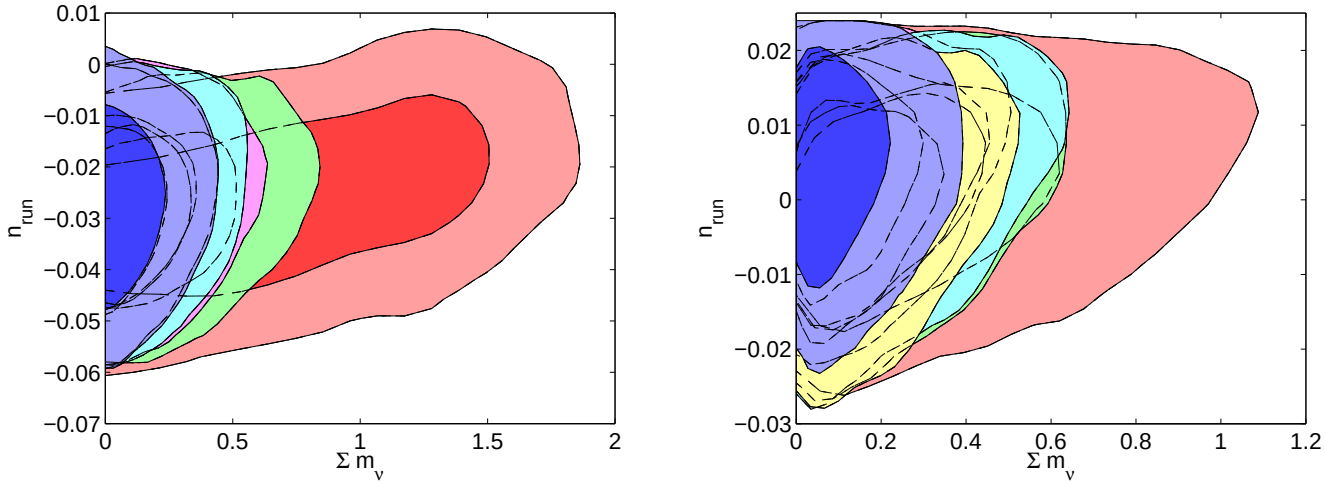

FIG. 4: Left panel (Three massive neutrino case plus $n_{\rm run}$): the red contours show the 68% and 95% CL allowed regions from the combination of WMAP and SPT measurements in the ($\sum m_\nu$ (eV), $n_{\rm run}$) plane, while the magenta (blue) ones show the impact of the addition of SNLS3 (HST) data sets. The green contours depict the results from the combination of CMB and BAO data, while the cyan and yellow ones show the impact of the SNLS3 (HST) data combined with CMB and BAO measurements. Right panel: as in the left panel but for the case of ACT data.

perfectly consistent and indicating both $N_{\rm eff} > 3$ at 1-2 standard deviations. The addition of SNLS3 data will not help much in improving the agreement between these two data sets, see Tabs. VI and VII, where we summarise the mean values and errors found for $N_{\rm eff}$ for the different data combinations considered here. Therefore, as in the three massive neutrino case, the consistency between ACT and SPT CMB results is greatly improved if BAO and HST data are considered as well.

D. Massive neutrinos and dark radiation

In this section we consider extended dark radiation cosmologies, parameterised via the dark radiation abundance $N_{\rm eff}$ and its clustering properties, represented by $c^2_{\rm eff}$ and $c^2_{\rm vis}$, see also Refs. [25–27] for bounds on these parameters within different cosmological models. Here three possible scenarios are examined. In the first scenario there are three massive neutrinos with $\sum m_\nu = 0.3$ eV, which roughly corresponds to the mean value obtained in Ref. [31], and $\Delta N_{\rm eff}$ massless neutrino species with $c^2_{\rm vis} = c^2_{\rm eff} = 1/3$. In the second scenario the clustering parameters of the dark radiation component are allowed to vary, as well as in the third scenario, in which also the sum pf the masses of the three massive neutrinos $\sum m_\nu$ varies. Our findings are summarised in Figs. 7 and 6, where we illustrate the constraints from SPT and ACT probes.

In the first scenario, in which both $c^2_{\rm eff}$ and $c^2_{\rm vis}$ are fixed to their standard values and assuming three massive neutrinos with $\sum m_\nu = 0.3$ eV, we find that $\Delta N_{\rm eff} = 0.89 \pm 0.56$ ($\Delta N_{\rm eff} = 0.42 \pm 0.34$) when considering WMAP plus SPT (ACT) measurements. When HST data are added in the analyses, the mean values of $\Delta N_{\rm eff}$ for these two probes are similar: $\Delta N_{\rm eff} = 0.95 \pm 0.42$ ($\Delta N_{\rm eff} = 0.71 \pm 0.40$) for WMAP, SPT and HST (WMAP, ACT and HST) measurements. The addition of BAO data does not improve the agreement between SPT and ACT.

In the second scenario, only $\sum m_\nu = 0.3$ eV remains as a fixed parameter. In this case, the discrepancy between SPT and ACT data sets is larger, being the mean values for $\Delta N_{\rm eff} = 1.31 \pm 0.60$ and $\Delta N_{\rm eff} = 0.38 \pm 0.32$ respectively. The addition of HST brings these two mean values closer, being $\Delta N_{\rm eff} = 0.92 \pm 0.39$ ($\Delta N_{\rm eff} = 0.62 \pm 0.41$) for the combinations of WMAP, SPT and HST (WMAP, ACT and HST) data sets. Concerning the values of the dark radiation clustering parameters $c^2_{\rm eff}$ and $c^2_{\rm vis}$, we find that SPT data exclude the standard value of $c^2_{\rm vis} = 1/3$ at the 2σ CL. The mean value is $c^2_{\rm vis} = 0.15 \pm 0.07$ ($c^2_{\rm vis} < 0.28$ at 95% CL) when combining SPT, WMAP, BAO and HST data sets. The results for the effective speed of sound seem to be consistent with standard expectations, finding, for the same combination of data sets, that $c^2_{\rm eff} = 0.32 \pm 0.012$. Similar results are obtained when SPT data is combined with the other data sets considered here. However, the results of the analyses of ACT data provide values for the clustering parameters which perfectly agree with standard expectations, being $c^2_{\rm eff} = 0.35 \pm 0.02$ and $c^2_{\rm vis} = 0.25 \pm 0.13$ ($c^2_{\rm vis} < 0.61$ at 95% CL) for the analysis of ACT, WMAP, BAO and HST data sets.

In the third scenario, all four parameters $\Delta N_{\rm eff}$, $c^2_{\rm vis}$, $c^2_{\rm eff}$ and $\sum m_\nu$ are allowed to freely vary, and we depict the constraints arising from our analyses in Figs. 6. The evidence for neutrino masses when analysing SPT data gets diluted for all the data combinations except when BAO data is also added in the analyses. We find $\Delta N_{\rm eff} =$

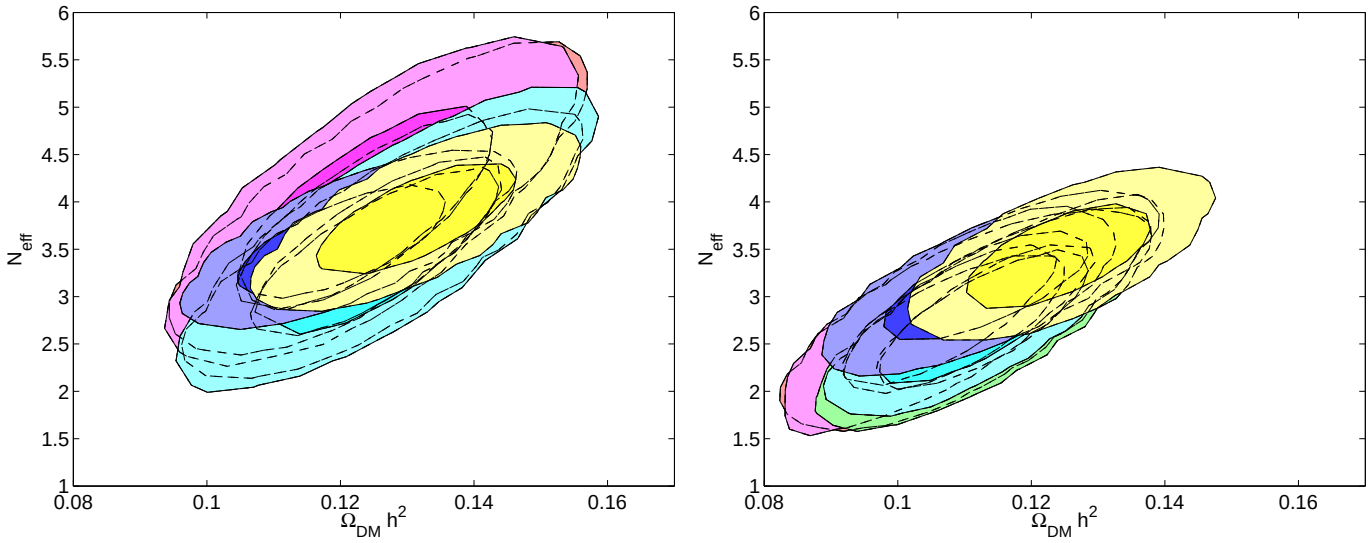

FIG. 5: Left panel (Massless neutrino case): the red contours show the 68% and 95% CL allowed regions from the combination of WMAP and SPT measurements in the ($\Omega_{\rm dm}h^2$, $N_{\rm eff}$) plane, while the magenta (blue) ones show the impact of the addition of SNLS3 (HST) data sets. The green contours depict the results from the combination of CMB and BAO data, while the cyan and yellow ones show the impact of the SNLS3 (HST) data combined with CMB and BAO measurements. Right panel: as in the left panel but considering ACT data instead of SPT CMB data.

	W9+SPT	W9+SPT + HST	W9+SPT +BAO	W9+SPT +SNLS3	W9+SPT +BAO+HST	W9+SPT +BAO+SNLS3
$N_{\rm eff}$	3.93 ± 0.68	3.59 ± 0.39	3.50 ± 0.59	3.96 ± 0.69	3.83 ± 0.41	3.55 ± 0.63

TABLE VI: Mean values and errors on $N_{\rm eff}$ in a standard cosmology with $N_{\rm eff}$ massless neutrinos for the different combinations of data sets in the case of considering high multipole data from SPT.

1.34 ± 0.67, ($\Delta N_{\rm eff} = 1.15 \pm 0.64$) and $\sum m_\nu < 1.3$ eV ($\sum m_\nu < 1.75$ eV) at 95% CL when considering CMB (CMB plus HST) measurements. For the combination of WMAP, SPT and BAO (WMAP, SPT, BAO and HST) data sets, the cosmological evidence for neutrino masses still remains, finding that $\Delta N_{\rm eff} = 1.30 \pm 0.77$ ($\Delta N_{\rm eff} = 1.35 \pm 0.50$) and $\sum m_\nu = 0.68 \pm 0.31$ eV ($\sum m_\nu = 0.67 \pm 0.29$ eV). When analysing ACT data (see right panel of Fig. 6) the bounds on both $\Delta N_{\rm eff}$ and $\sum m_\nu$ are tighter than those found for SPT data. For the combination of WMAP, ACT, HST and BAO data sets, $\Delta N_{\rm eff} = 0.74 \pm 0.40$ and $\sum m_\nu < 0.46$ eV at 95% CL. Regarding the values of $c^2_{\rm eff}$ and $c^2_{\rm vis}$, we find very similar results to those shown previously. In this third scenario in which the sum of the three massive neutrinos is also a free parameter, we find that SPT data again exclude the standard value of $c^2_{\rm vis} = 1/3$ at the 2σ CL, while the value of $c^2_{\rm eff}$ agrees with its standard prediction. The analysis of SPT, WMAP, BAO and HST gives $c^2_{\rm vis} = 0.13 \pm 0.07$ ($c^2_{\rm vis} < 0.26$ at 95% CL) and $c^2_{\rm eff} = 0.32 \pm 0.01$. In the case of ACT data, the values for both clustering parameters perfectly agree with standard expectations, being $c^2_{\rm eff} = 0.35 \pm 0.02$ and $c^2_{\rm vis} = 0.25 \pm 0.11$ ($c^2_{\rm vis} < 0.47$ at 95% CL) for the analysis of ACT, WMAP, BAO and HST data sets.

Figure 7, left (right) panel, shows the constraints on the dark radiation abundance versus the effective speed of sound (viscosity parameter) for the combination of SPT or ACT with WMAP, BAO and HST measurements. Note that SPT and ACT data seem to be again in disagreement, this time concerning the dark radiation clustering parameter $c^2_{\rm vis}$.

IV. CONCLUSIONS

New Cosmic Microwave Background measurements have become recently available, motivating us to explore the improvements in the measurements of the properties of the cosmic neutrino and dark radiation backgrounds. Interestingly, the new measurements of the CMB damping tail from the South Pole Telescope, SPT, and from the Atacama Cosmology Telescope, ACT, seem to give different results concerning neutrino masses and abundances. While the SPT collaboration finds $\sim 3\sigma$ evidence for neutrino masses and $N_{\rm eff} > 3$ at $\sim 2\sigma$, the ACT collaboration does not find evidence for neutrino masses and

	W9+ACT	W9+ACT + HST	W9+ACT +BAO	W9+ACT +SNLS3	W9+ACT +BAO+HST	W9+ACT +BAO+SNLS3
$N_{\rm eff}$	2.74 ± 0.47	3.12 ± 0.38	2.77 ± 0.49	2.79 ± 0.47	3.43 ± 0.36	2.83 ± 0.47

TABLE VII: Mean values and errors on $N_{\rm eff}$ in a standard cosmology with $N_{\rm eff}$ massless neutrinos for the different combinations of data sets in the case of considering high multipole data from ACT.

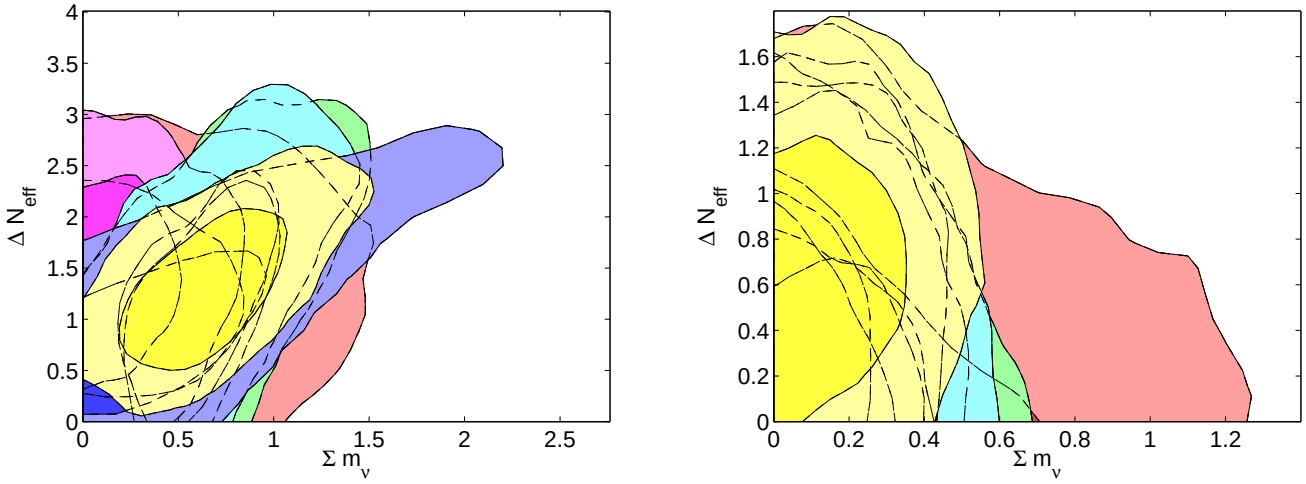

FIG. 6: Left panel ($\Delta N_{\rm eff}$ dark radiation species plus three massive neutrinos): the red contours show the 68% and 95% CL allowed regions from the combination of WMAP and SPT measurements in the ($\sum m_\nu$ (eV), $\Delta N_{\rm eff}$) plane, while the magenta (blue) ones show the impact of the addition of SNLS3 (HST) data sets. The green contours depict the results from the combination of CMB and BAO data, while the cyan and yellow ones show the impact of the SNLS3 (HST) data combined with CMB and BAO measurements. Right panel: as in the left panel but considering ACT measurements instead of SPT data.

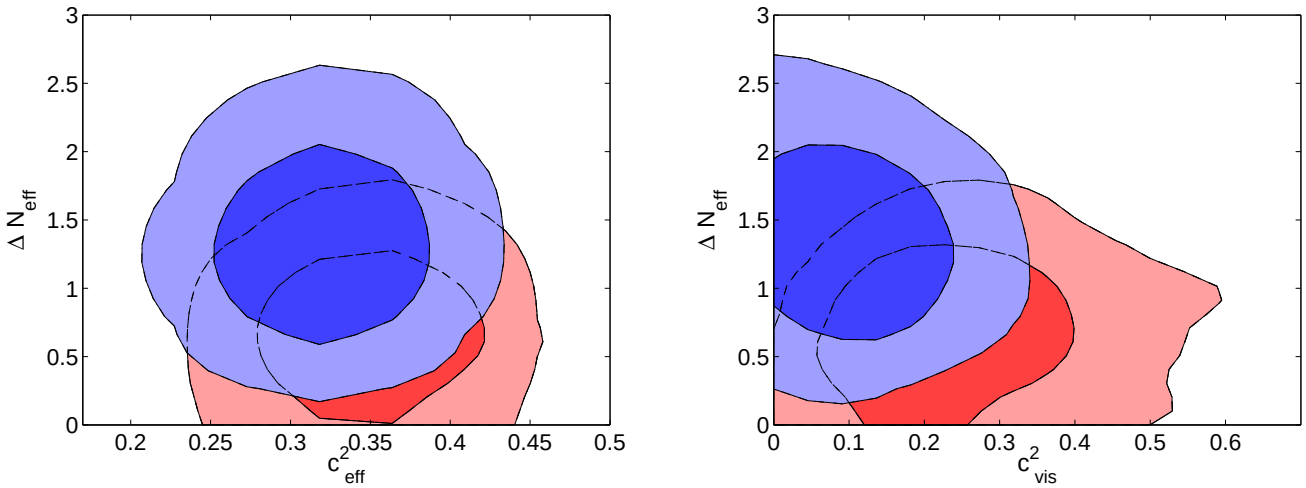

FIG. 7: Left panel ($\Delta N_{\rm eff}$ massless neutrinos and three massive with $\sum m_\nu = 0.3$ eV): the red (blue) contours show the 68% and 95% CL allowed regions from the combination of WMAP, SPT (ACT), BAO and HST measurements in the ($c^2_{\rm eff}$, $\Delta N_{\rm eff}$) plane. Right panel: as in the left panel but in the ($c^2_{\rm vis}$, $\Delta N_{\rm eff}$) plane.

their value for $N_{\rm eff}$ is much lower, agreeing perfectly with the standard model prediction of $N_{\rm eff} = 3$. The success of future Majorana neutrino searches relies on the absolute scale of neutrino masses; therefore a detailed analysis of both data sets separately combined with other cosmological measurements is mandatory. We have considered the most recent Baryon Acoustic Oscillation data, measurements of the Hubble constant from the Hubble Space Telescope, as well as Supernovae Ia luminosity distance measurements. In the standard ΛCDM scenario with either three massive neutrino species or $N_{\rm eff}$ massless species, the results from the two high CMB multiple probes are consistent if Baryon Acoustic Oscillation data is removed from the analyses and a prior on H_0 from HST is also considered. In the case of $N_{\rm eff}$ massive neutrino species, SPT and ACT data analyses give very different results for $\sum m_\nu$: while the evidence for $\sum m_\nu \sim 0.5$ eV found for SPT data persists independently of the data sets combined, the ACT data provide a 95% CL upper bound of ~ 0.4 eV on $\sum m_\nu$. We then explore extended cosmologies models, finding that, in general, the SPT data evidence for neutrino masses found in the minimal ΛCDM scenario gets diluted except for the case of a dark radiation background of unknown clustering properties with BAO data included. In the former case, SPT data exclude the standard value for the viscosity parameter of the dark radiation fluid $c^2_{\rm vis} = 1/3$ at the 2σ CL, regardless of the data sets considered in the analysis. Upcoming, high precision CMB data from the Planck satellite will help in disentangling the high tail CMB neutrino–dark radiation puzzle.

V. ACKNOWLEDGMENTS

O.M. is supported by the Consolider Ingenio project CSD2007-00060, by PROMETEO/2009/116, by the Spanish Ministry Science project FPA2011-29678 and by the ITN Invisibles PITN-GA-2011-289442. MA acknowledges the European ITN project Invisibles (FP7-PEOPLE-2011-ITN, PITN-GA-2011-289442-INVISIBLES).

[1] S. Hannestad, A. Mirizzi, G. G. Raffelt and Y. Y. Y. Wong, JCAP **1008** (2010) 001 [arXiv:1004.0695 [astro-ph.CO]]; A. Melchiorri, O. Mena and A. Slosar, Phys. Rev. D **76** (2007) 041303 [arXiv:0705.2695 [astro-ph]].
[2] W. Fischler, J. Meyers, Phys. Rev. **D83** (2011) 063520. [arXiv:1011.3501 [astro-ph.CO]].
[3] T. L. Smith, E. Pierpaoli and M. Kamionkowski, Phys. Rev. Lett. **97** (2006) 021301 [arXiv:astro-ph/0603144].
[4] P. Binetruy, C. Deffayet, U. Ellwanger and D. Langlois, Phys. Lett. B **477** (2000) 285 [arXiv:hep-th/9910219]; T. Shiromizu, K. i. Maeda and M. Sasaki, Phys. Rev. D **62** (2000) 024012 [arXiv:gr-qc/9910076]; V. V. Flambaum and E. V. Shuryak, Europhys. Lett. **74** (2006) 813 [arXiv:hep-th/0512038].
[5] E. Calabrese, D. Huterer, E. V. Linder, A. Melchiorri and L. Pagano, Phys. Rev. D **83**, 123504 (2011) [arXiv:1103.4132 [astro-ph.CO]].
[6] M. Blennow, E. Fernandez-Martinez, O. Mena, J. Redondo and P. Serra, JCAP **1207**, 022 (2012) [arXiv:1203.5803 [hep-ph]].
[7] G. Mangano, A. Melchiorri, O. Mena, G. Miele and A. Slosar, JCAP **0703**, 006 (2007) [arXiv:astro-ph/0612150].
[8] J. Hamann, S. Hannestad, G. G. Raffelt and Y. Y. Y. Wong, JCAP **0708**, 021 (2007) [arXiv:0705.0440 [astro-ph]].
[9] M. A. Acero and J. Lesgourgues, Phys. Rev. D **79** (2009) 045026 [arXiv:0812.2249 [astro-ph]].
[10] A. Melchiorri, O. Mena, S. Palomares-Ruiz, S. Pascoli, A. Slosar and M. Sorel, JCAP **0901**, 036 (2009) [arXiv:0810.5133 [hep-ph]].
[11] B. A. Reid, L. Verde, R. Jimenez and O. Mena, JCAP **1001**, 003 (2010) [arXiv:0910.0008 [astro-ph.CO]].
[12] J. Hamann, S. Hannestad, J. Lesgourgues, C. Rampf and Y. Y. Y. Wong, JCAP **1007**, 022 (2010) [arXiv:1003.3999 [astro-ph.CO]].
[13] J. Hamann, S. Hannestad, G. G. Raffelt, I. Tamborra and Y. Y. Y. Wong, Phys. Rev. Lett. **105**, 181301 (2010) [arXiv:1006.5276 [hep-ph]].
[14] E. Giusarma, M. Corsi, M. Archidiacono, R. de Putter, A. Melchiorri, O. Mena, S. Pandolfi, Phys. Rev. **D83**, 115023 (2011). [arXiv:1102.4774 [astro-ph.CO]].
[15] Z. Hou, R. Keisler, L. Knox, M. Millea and C. Reichardt, arXiv:1104.2333 [astro-ph.CO].
[16] J. Hamann, S. Hannestad, G. G. Raffelt, Y. Y. Y. Wong, JCAP **1109**, 034 (2011). [arXiv:1108.4136 [astro-ph.CO]].
[17] J. Hamann, JCAP **1203**, 021 (2012) [arXiv:1110.4271 [astro-ph.CO]].
[18] K. M. Nollett and G. P. Holder, arXiv:1112.2683 [astro-ph.CO].
[19] E. Giusarma, M. Archidiacono, R. de Putter, A. Melchiorri and O. Mena, Phys. Rev. D **85**, 083522 (2012) [arXiv:1112.4661 [astro-ph.CO]].
[20] R. de Putter, O. Mena, E. Giusarma, S. Ho, A. Cuesta, H. -J. Seo, A. Ross and M. White *et al.*, arXiv:1201.1909 [astro-ph.CO].
[21] S. Joudaki, K. N. Abazajian and M. Kaplinghat, arXiv:1208.4354 [astro-ph.CO].
[22] S. Riemer-Sorensen, D. Parkinson, T. Davis and C. Blake, arXiv:1210.2131 [astro-ph.CO].
[23] E. Giusarma, R. de Putter and O. Mena, arXiv:1211.2154 [astro-ph.CO].
[24] M. Archidiacono, N. Fornengo, C. Giunti, S. Hannestad and A. Melchiorri, arXiv:1302.6720 [astro-ph.CO].
[25] R. Diamanti, E. Giusarma, O. Mena, M. Archidiacono and A. Melchiorri, arXiv:1212.6007 [astro-ph.CO].
[26] M. Archidiacono, E. Giusarma, A. Melchiorri and O. Mena, Phys. Rev. D **86** (2012) 043509

[arXiv:1206.0109 [astro-ph.CO]].
[27] M. Archidiacono, E. Calabrese and A. Melchiorri, Phys. Rev. D **84** (2011) 123008 [arXiv:1109.2767 [astro-ph.CO]].
[28] G. Hinshaw, D. Larson, E. Komatsu, D. N. Spergel, C. L. Bennett, J. Dunkley, M. R. Nolta and M. Halpern *et al.*, arXiv:1212.5226 [astro-ph.CO].
[29] S. Das, B. D. Sherwin, P. Aguirre, J. W. Appel, J. R. Bond, C. S. Carvalho, M. J. Devlin and J. Dunkley *et al.*, Phys. Rev. Lett. **107**, 021301 (2011) [arXiv:1103.2124 [astro-ph.CO]].
[30] R. Keisler, C. L. Reichardt, K. A. Aird, B. A. Benson, L. E. Bleem, J. E. Carlstrom, C. L. Chang and H. M. Cho *et al.*, Astrophys. J. **743**, 28 (2011) [arXiv:1105.3182 [astro-ph.CO]].
[31] Z. Hou, C. L. Reichardt, K. T. Story, B. Follin, R. Keisler, K. A. Aird, B. A. Benson and L. E. Bleem *et al.*, arXiv:1212.6267 [astro-ph.CO].
[32] K. T. Story, C. L. Reichardt, Z. Hou, R. Keisler, K. A. Aird, B. A. Benson, L. E. Bleem and J. E. Carlstrom *et al.*, arXiv:1210.7231 [astro-ph.CO].
[33] P. A. R. Ade *et al.* [Planck Collaboration], Astron. Astrophys. **536**, 16464 (2011) [arXiv:1101.2022 [astro-ph.IM]].
[34] J. J. Gomez-Cadenas, J. Martin-Albo, J. M. Vidal and C. Pena-Garay, arXiv:1301.2901 [hep-ph].
[35] J. L. Sievers, R. A. Hlozek, M. R. Nolta, V. Acquaviva, G. E. Addison, P. A. R. Ade, P. Aguirre and M. Amiri *et al.*, arXiv:1301.0824 [astro-ph.CO].
[36] E. Di Valentino, S. Galli, M. Lattanzi, A. Melchiorri, P. Natoli, L. Pagano and N. Said, arXiv:1301.7343 [astro-ph.CO].
[37] A. Lewis, A. Challinor and A. Lasenby, Astrophys. J. **538**, 473 (2000) [arXiv:astro-ph/9911177].
[38] A. Lewis and S. Bridle, Phys. Rev. D **66**, 103511 (2002) [arXiv:astro-ph/0205436].
[39] A. G. Riess, L. Macri, S. Casertano, H. Lampeitl, H. C. Ferguson, A. V. Filippenko, S. W. Jha and W. Li *et al.*, Astrophys. J. **730**, 119 (2011) [Erratum-ibid. **732**, 129 (2011)] [arXiv:1103.2976 [astro-ph.CO]].
[40] A. Conley *et al.*, Astrophys. J. Suppl. **192**, 1 (2011) [arXiv:1104.1443 [astro-ph.CO]].
[41] L. Anderson *et al.*, arXiv:1203.6594 [astro-ph.CO].
[42] D. Schlegel *et al.* [with input from the SDSS-III Collaboration], arXiv:0902.4680 [astro-ph.CO].
[43] K. S. Dawson *et al*, arXiv:1208.0022 [astro-ph.CO].
[44] D. J. Eisenstein *et al.*, Astrophys. J. **664**, 675 (2007) [arXiv:astro-ph/0604362.
[45] N. Padmanabhan, X. Xu, D. J. Eisenstein, R. Scalzo, A. J. Cuesta, K. T. Mehta and E. Kazin, arXiv:1202.0090 [astro-ph.CO].
[46] F. Beutler *et al.*, Mon. Not. Roy. Astron. Soc. **416**, 3017 (2011) [arXiv:1106.3366 [astro-ph.CO]].
[47] C. Blake, E. Kazin, F. Beutler, T. Davis, D. Parkinson, S. Brough, M. Colless and C. Contreras *et al.*, Mon. Not. Roy. Astron. Soc. **418**, 1707 (2011) [arXiv:1108.2635 [astro-ph.CO]].
[48] S. Hannestad, Phys. Rev. Lett. **95**, 221301 (2005) [astro-ph/0505551].
[49] A. Kosowsky and M. S. Turner, Phys. Rev. D **52**, 1739 (1995) [astro-ph/9504071].